CLINICAL ARTICLE

Titanium Alloy Gamma Nail *versus* Biodegradable Magnesium Alloy Bionic Gamma Nail for Treating Intertrochanteric Fractures: A Finite Element Analysis

Ming Li, MD[1†], Kuo Zhao, MD[1†], Kai Ding, MD[1], Yun-wei Cui, MD[1], Xiao-dong Cheng, MD[1,2], Wei-jie Yang, MD[1], Zhi-yong Hou, MD[1], Ying-ze Zhang, MD[1,2], Wei Chen, MD[1,2], Pan Hu, MD[3], Yan-bin Zhu, MD[1,2]

[1]*Department of Orthopaedic Surgery, The Third Hospital of Hebei Medical University and* [2]*Key Laboratory of Biomechanics of Hebei Province, Shijiazhuang and* [3]*Department of Orthopaedic Surgery, The Peking University People's Hospital, Beijing, China*

Objective: To using finite element analysis to investigate the effects of the traditional titanium alloy Gamma nail and a biodegradable magnesium alloy bionic Gamma nail for treating intertrochanteric fractures.

Methods: Computed tomography images of an adult male volunteer of appropriate age and in good physical condition were used to establish a three-dimensional model of the proximal femur. Then, a model of a type 31A1 intertrochanteric fracture of the proximal femur was established, and the traditional titanium alloy Gamma nails and biodegradable magnesium alloy bionic Gamma nails were used for fixation, respectively. The von Mises stress, the maximum principal stress, and the minimum principal stress were calculated to evaluate the effect of bone ingrowth on stress distribution of the proximal femur after fixation.

Results: In the intact model, the maximum stress was 5.8 MPa, the minimum stress was −11.7 MPa, and the von Mises stress was 11.4 MPa. The maximum principal stress distribution of the cancellous bone in the intact model appears in a position consistent with the growth direction of the principal and secondary tensile zones. After traditional Gamma nail healing, the maximum stress was 32 MPa, the minimum stress was −23.5 MPa, and the von Mises stress was 31.3 MPa. The stress concentration was quite obvious compared with the intact model. It was assumed that the nail would biodegrade completely within 12 months postoperatively. The maximum stress was 18.7 MPa, the minimum stress was −12.6 MPa, and the von Mises stress was 14.0 MPa. For the minimum principal stress, the region of minimum stress value less than −10 MPa was significantly improved compared with the traditional titanium alloy Gamma nail models. Meanwhile, the stress distribution of the bionic Gamma nail model in the proximal femur was closer to that of the intact bone, which significantly reduced the stress concentration of the implant.

Conclusion: The biodegradable magnesium alloy bionic Gamma nail implant can improve the stress distribution of fractured bone close to that of intact bone while reducing the risk of postoperative complications associated with traditional internal fixation techniques, and it has promising clinical value in the future.

Key words: Bionic internal fixation; Finite element analysis; Gamma nail; Intertrochanteric fracture; Trabecular bone

Address for correspondence Wei Chen, MD, Department of Orthopaedic Surgery, The Third Hospital of Hebei Medical University, 139 Ziqiang Road, Qiaoxi District, Shijiazhuang, China 050051 Phone: +86 18533112839, Fax: +86 311 88603000; Email: drchenwei1@163.com; or Pan Hu, MD, Department of Orthopaedic Surgery, The Peking University People's Hospital, No. 11 Xizhimen South Street, Beijing, China 100044; Email: panhu_1989@163.com; or Yan-bin Zhu, MD, Department of Orthopaedic Surgery, The Third Hospital of Hebei Medical University, 139 Ziqiang Road, Qiaoxi District, Shijiazhuang, China 050051 Phone: +86 13931170702; Fax: +86 311 88603000; Email: zhuyanbin111@126.com
[†]These authors contributed equally to this work.

Grant Sources: This study was supported by the Foundation for Innovative Research Groups of the National Natural Science Foundation of China (Grant No. 82072447, 81401789), the Natural Science Foundation of Hebei Province (CN) -Outstanding Youth Foundation (Grant No. H2017206104).
Disclosure: The authors have no conflict of interest to declare.
Received 16 August 2020; accepted 29 November 2020

Introduction

Hip fractures are common in the elderly. It is estimated that in 2050, there will be 6.3 million hip fractures worldwide, with approximately 90% occurring in people above 65 years of age and approximately 50% being intertrochanteric fractures[1–4]. Intertrochanteric fractures account for approximately 3.40% of all fractures in adults and are associated with the risk of many complications and even death[5–9]. The intertrochanteric fracture-related mortality rate is as high as 30% in the first 12 months after injury, especially in the elderly with limited mobility[10]. Therefore, it is an important task for orthopaedic trauma surgeons to study the causes, mechanisms, and methods of internal fixation of intertrochanteric fractures to improve the therapeutic effects and reduce complications.

Currently, patients with intertrochanteric fractures are mainly treated surgically. The commonly used instruments in such surgeries include dynamic hip screws (DHS), Gamma nails, and proximal femoral nail anti-rotation (PFNA)[11–13]. The continuous advancement of internal fixation devices and surgical techniques has improved the therapeutic effect of intertrochanteric fractures. However, implants can further destroy the trabecular bone structure during the healing process. The trabecular bone is hindered due to screw fixation and its continuity cannot be restored. Even if the cortical bone has healed, the load on the femoral head cannot be transmitted as normal[14]. Therefore, local stress concentration can occur, resulting in internal fixator loosening, exiting, fracture nonunion, and other complications. The failure rate of DHS, Gamma nails, and PFNA fixation for intertrochanteric fractures ranges from 8% to 56%[15–17]. Horner *et al.*[18] evaluated 644 patients who received long or short Gamma nails for hip fractures and found that 9.8% of patients had surgical complications. Huang *et al.*[19] used Gamma nails in 186 patients for surgical treatment, and found that lag screws were more likely to come out in cases of osteoporosis and premature loading. In addition, invasive secondary surgery is often required to remove the internal fixation material after the fracture has completely healed, which not only results in more pain and clinical risks for the patient but also increases the financial burden on patients.

Considering the limitations of the traditional Gamma nail structure, we developed a biodegradable magnesium alloy porous bionic Gamma nail (Fig. 1). The purpose of the present study was to: (i) construct a three-dimensional model of the proximal femur that simulated human reality; (ii) compare the stress distribution of traditional titanium alloy and magnesium alloy Gamma nail fixation for treatment of intertrochanteric fractures using finite element analysis; and (iii) observe the efficiency of the biodegradable magnesium alloy bionic Gamma nail for treating intertrochanteric fractures.

Materials and Methods

This study was reviewed and approved by the Institutional Review Board of the Third Hospital of Hebei Medical

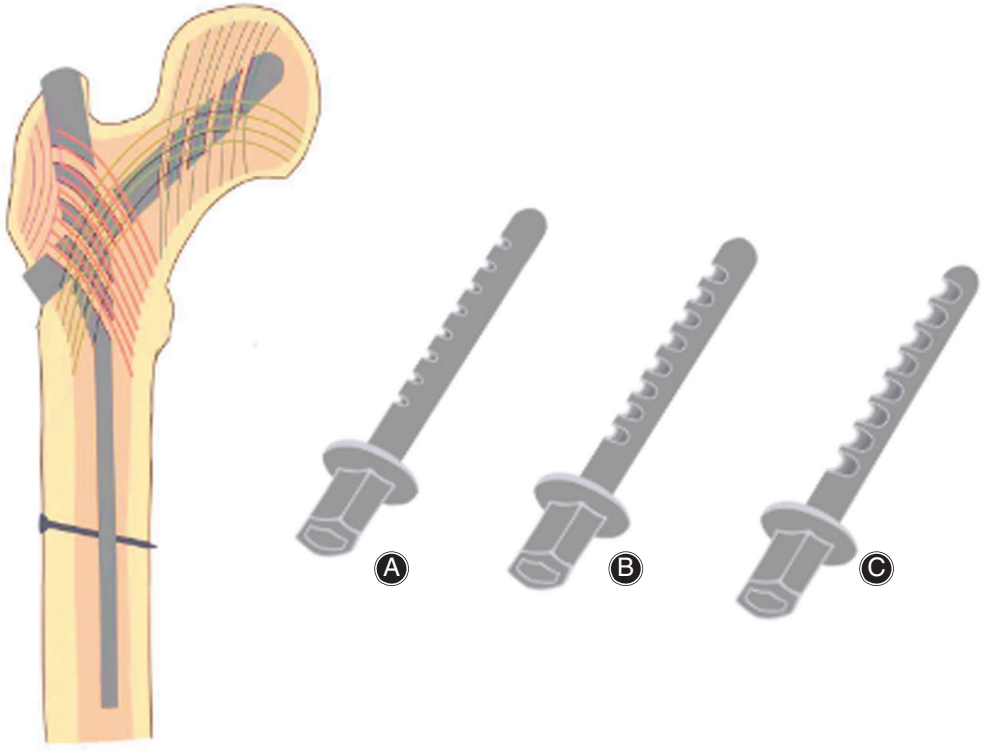

Fig. 1 Schematic diagram of bionic holes with different diameters on bionic Gamma nails and lag screws: (A) small aperture, (B) medium aperture, and (C) large aperture.

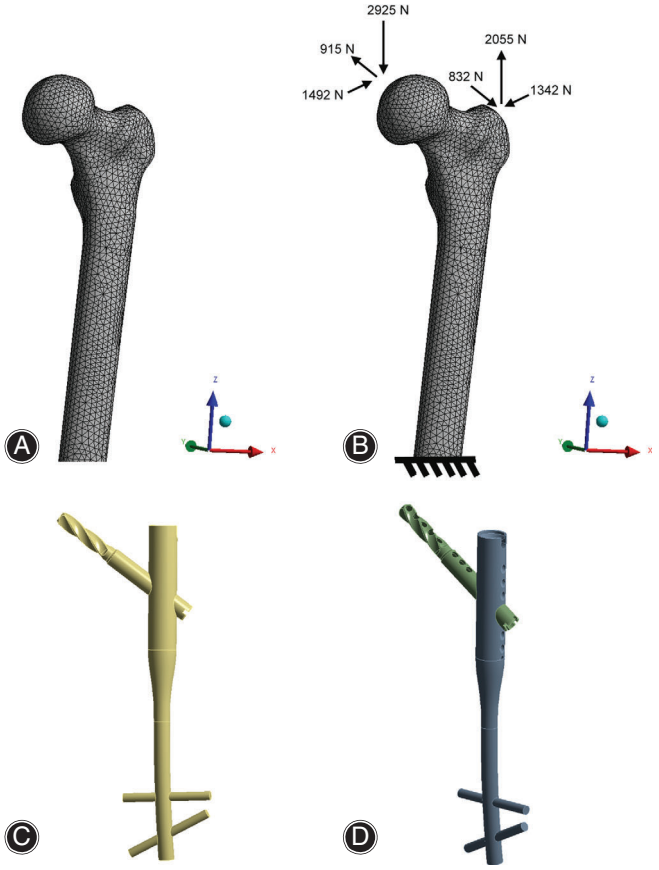

Fig. 2 (A) Meshed model of the proximal femur. (B) Loading was modeled. (C) Model of traditional Gamma nails. (D) Model of bionic Gamma nails.

University and conforms to the provisions of the Declaration of Helsinki. Written informed consent was obtained from the patient prior to the commencement of the study.

Establishment of the Gamma Nail Models

First, the traditional three-dimensional numerical model of the Gamma nail was established (Fig. 2C), and then small holes (Fig. 2D) were added to the lag screw of the Gamma nail. This nail that we developed is characterized by a hollow structure and many holes on the surface connected to the internal space, with the purpose of allowing cancellous bone for growth into the screw.

Establishment of the Finite Element Models of the Proximal Femur

A 35-year-old male volunteer was selected and examined with radiograph scanning to exclude deformity in his hip. The volunteer stood at a height of 176 cm and weighed 65 kg. A three-dimensional solid proximal femur model was constructed using human CT images for this analysis, including cortical and cancellous bones. A model of a type 31A1 intertrochanteric fracture of the proximal femur was established and fixed with traditional and bionic Gamma nails, respectively (Fig. 3).

The three-dimensional numerical model was imported into ANSYS Workbench 14.5 to establish the finite element model. The intact femur model is shown in Fig. 2A. Bone was defined based on linear elastic material properties. Young's modulus of cortical bone was 17 GPa, and that of cancellous bone was 1.5 Gpa. Poisson's ratio for both cortical and cancellous bones was 0.3[20].

Young's modulus of the traditional and the biodegradable Gamma nail was 110 and 45 GPa, respectively, and Poisson's ratio was 0.316 (Table 1). All materials were assumed to be homogeneous, isotropic, and to have linear elastic behavior. The contact characteristics between the screw and the cancellous bone and the cortical bone were assumed to be fully bonding, and the contact surface of the other parts was assumed to be frictional contact. The coefficient of friction was set at 0.3[21].

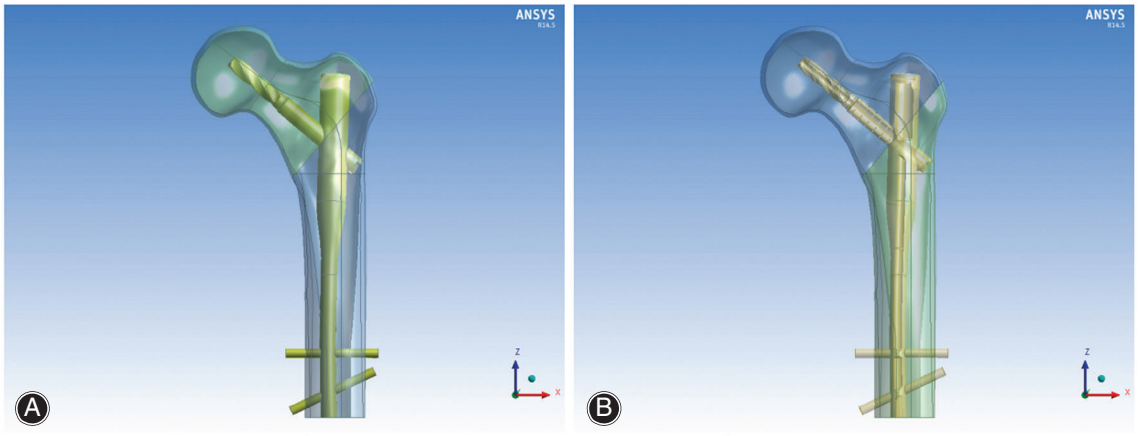

Fig. 3 A model of the type 31A1 intertrochanteric fracture of the proximal femur was established and implanted with the traditional Gamma nail (A) and bionic Gamma nail (B).

TABLE 1 Material properties of all modes in this study

Model	Materials	Young's modulus (GPa)	Poisson's ratio
Cortical bone	Cortical bone	17	0.3
Cancellous	Cancellous bone	1.5	0.3
Traditional Gamma nail	Ti6Al4V	110	0.316
Biodegradable Gamma nail	Mg alloy	45	0.316
Biodegradable Gamma nail (PO 12 months)	Mg alloy	9	0.316

Note: PO, postoperative.

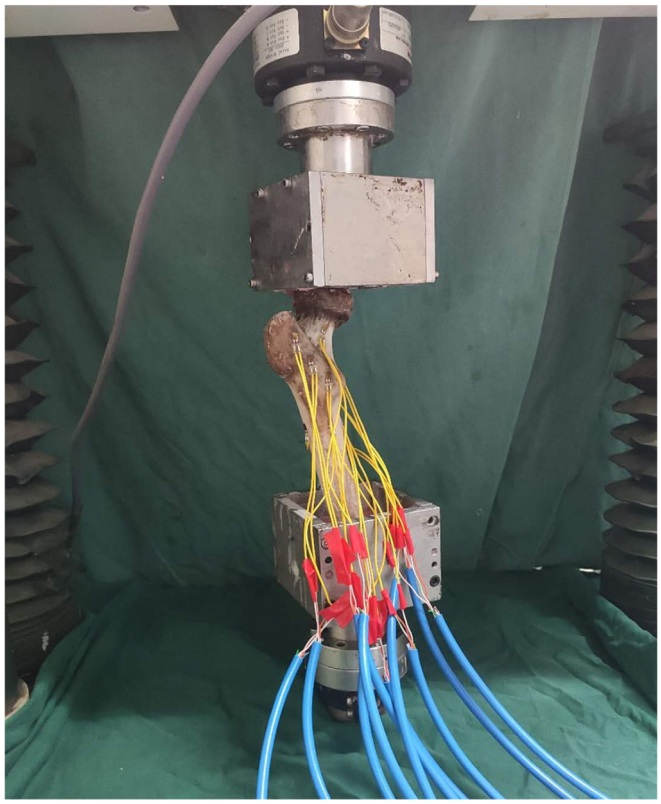

Fig. 4 A sample of a normal proximal femur was selected for a biomechanical test. Nine marker points were selected to paste strain gauge on the solid specimen, and then 750 N load was applied to the femur specimen to record the strain value of the marker points.

Assuming that the average weight of the patient was 750 N, the loading force acting on the femur constitutes the load when the heel strikes during normal walking[22]. Figure 2B shows the head load ($\{x, y, z\}$ = {1492, 915, −2925} N) and abductor force ($\{x, y, z\}$ = {−1342, −832, 2055} N) (4.54 and 3.45 times body weight, respectively). The lateral femur is in the positive x-axis direction, the posterior femur is in the positive y-axis direction, and the proximal femur is in the positive z-axis direction.

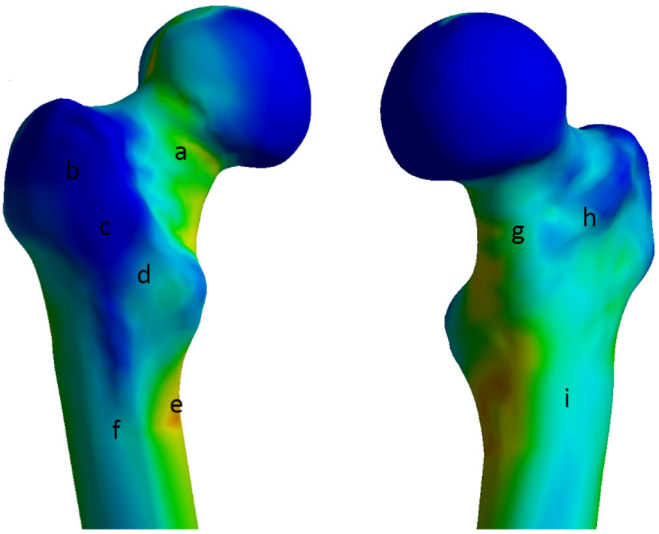

Fig. 5 The same loading conditions and boundary conditions were applied for finite element analysis.

Model Validation

To verify the proximal femur finite element model, a sample of a normal proximal femur was selected for biomechanical testing (Fig. 4). Nine marker points were selected to paste strain gauge on solid specimens and then a 750 N load was applied to the femur specimen to record the strain value of marker points. The same loading conditions and boundary conditions were applied for finite element analysis (Fig. 5). The results of the biomechanical test and finite element analysis were compared to validate the finite element model (Table 2).

The three-dimensional solid model of the proximal femur used in this analysis was established with human CT images and validated in our previous study[23]. In addition, the von Mises stress on the cancellous and cortical bone in the intact femur was tested to analyze the mesh convergence and validate the model in this study. The convergence criterion used was a change less than 5% (Fig. 6), under a loading of 750 N, as shown in Fig. 2B. The final model had 62,374 elements (22,137 elements in cortical bone and 40,237 elements in cancellous bone, respectively).

TABLE 2 The strain values of the biomechanical test and finite element analysis ($\times 10^{-3}$)

Maker point	a	b	c	d	e	f	g	h	i
Finite element analysis	4.24	0.02	0.04	1.40	6.53	2.40	5.02	2.52	2.97
Biomechanical test	4.43	0.02	0.04	1.53	6.82	2.75	5.27	2.45	2.67

Evaluation of Stress Distribution of Cancellous Bone in Proximal Femur

We assumed that the fracture had fully healed and that the contact conditions at the fracture surface were free of slip and separation. Ingrowth of bone was considered within the implant and through the holes. To compare the stress path of the trabecular bone in the implanted model and the intact model, the von Mises stress, the maximum principal stress, and the minimum principal stress were measured to evaluate the effect of bone ingrowth on the stress distribution of the cancellous bone in the proximal femur.

Results

Stress Distribution of Intact Bone

The distribution of the maximum principal stress of the cancellous bone in the intact model was consistent with the growth direction of primary and secondary tensile zones (Fig. 7A). The maximum stress was 5.8 MPa, and an area greater than 5 MPa was located under the greater trochanter. The minimum stress value was −11.7 MPa (Fig. 7B), with the stress area less than −10 MPa located above the femoral head. The minimum principal stress distribution of the finite element model was the same as that of the principal pressure zone of the trabecular bone. The von Mises stress distribution of the intact model with maximum stress was 11.4 MPa (Fig. 7C).

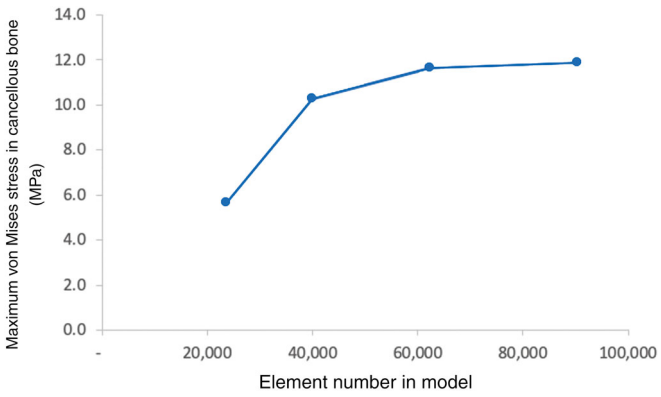

Fig. 6 The von Mises stress on the cancellous and cortical bone of the intact femur was tested to analyze the mesh convergence and validate the model.

Stress Distribution of the Traditional Gamma Nail Model

Figure 6 shows the distribution of the maximum principal stress, the minimum principal stress, and the von Mises stress after traditional Gamma nail healing. Comparing the maximum principal stress of the traditional Gamma nail (Fig. 8A) with the intact model (Fig. 7A), we found that the maximum stress was 32 MPa (more than 5 MPa), located at the junction of the anti-rotation screw and the main screw. While the minimum stress was −23.5 MPa, the area with a minimum stress value less than −10 MPa was located at the junction of anti-rotation screws and bolts and above the screw teeth. The von Mises stress distribution of the intact model with maximum stress was 31.3 MPa; the stress concentration was quite obvious compared with the intact model.

Stress Distribution of the Biodegradable Magnesium Alloy Bionic Gamma Nail Fixation Model

Figure 9 shows the maximum principal stress, the minimum principal stress, and the von Mises stress distributions for the biodegradable magnesium alloy bionic Gamma screw fixation model at 12 months after bone healing, assuming an 80% reduction in Young's modulus of implants (9 GPa). The maximum stress was 18.7 MPa, the minimum stress was −12.6 MPa, and the von Mises stress was 14 MPa, respectively. In the minimum principal stress, the region of minimum stress value less than −10 MPa was significantly improved compared with the traditional titanium alloy Gamma nail models. The minimum stress distribution of cancellous bone in the stress zone was close to that of intact bone due to decreased implant stiffness. In addition, compared with the traditional Gamma nails, the overall stress distribution of the biomimetic implant was closer to that of the complete bone, which significantly reduced the stress concentration of the implant.

Discussion

Role of Trabecular Bone at the Proximal Femur

The proximal femur has a truss structure composed of compressive trabecular bone, tensile trabecular bone, and calcar[24–26]. Due to the special anatomical structure, the body load is transmitted downward through the femoral head, resulting in a large bending moment. The proximal femoral intramedullary trabecular system can transform the bending moment, passing through the femoral head to the upper femur, making load bearing evenly distributed to the cortical bone. Finite element analysis based on μCT shows that trabecular bone bears 40%–70% of mechanical stress in the

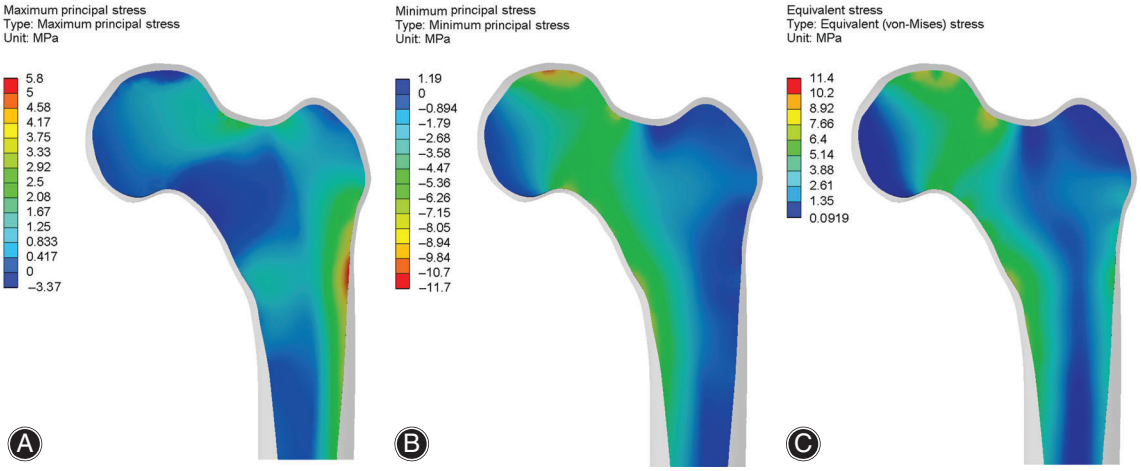

Fig. 7 Maximum principal stress distribution (A), minimum principal stress distribution (B), and von Mises stress distribution (C) of the intact bone.

femoral neck[27]. However, trabecular bone has an important "initial action" in the process of intertrochanteric fractures. The reduction of trabeculae and the decrease of bone density are important causes of intertrochanteric fractures in elderly patients[28]. Keaveny *et al.*[29] found that when the mechanical load is too high, tissue-level damage begins in the trabecular bone. Local high stress first causes part of the trabecular bone to break, which, in turn, causes the trabecular meshwork to break, and, finally, the cortical bone breaks (fracture). Therefore, reconstruction of the trabecular bone during fracture healing is essential to restore the mechanical support and conduction properties of the proximal femur.

Influence of Internal Fixation Device on Trabecular Bone

Although the commonly used internal fixation devices achieve good fixation, they have no function to protect and restore the trabecular bone. In addition to the damage to trabecular bone caused by fractures, internal fixation implants also destroy the main pressure, tension, and structure of the trabecular bone of the femoral moment and cause bone mass loss during their implanting process. Therefore, the "stress shielding" and volume-occupying effect at the late healing stage will hinder the reconstruction of trabecular bone, and its continuity cannot be restored, affecting the quality of healing[14]. Under the principle of biomechanics, the present study proposes a degradable magnesium alloy bionic Gamma nail system, whose main purpose is to reduce the rigidity of the implant, provide suitable conditions for the ingrowth of cancellous bone through the bionic hole, restore the original trabecular structures, and promote cortical-cancellous biphasic healing and restore mechanical support and conduction properties.

Advantages of Degradable Magnesium Alloys

In this study, the finite element model was used to compare the stress distribution of traditional titanium alloy Gamma

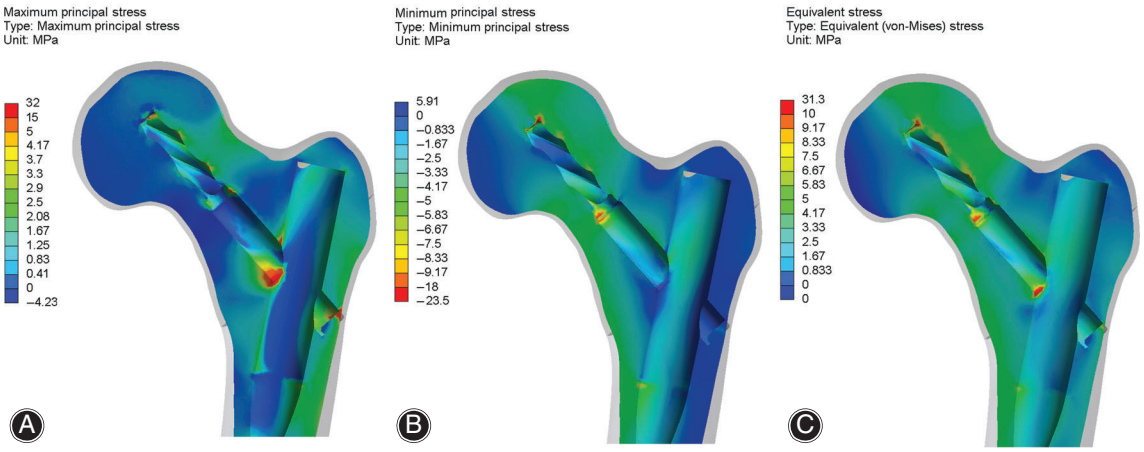

Fig. 8 Maximum principal stress distribution (A), minimum principal stress distribution (B), and von Mises stress distribution (C) of the proximal femur model implanted with traditional Gamma nail.

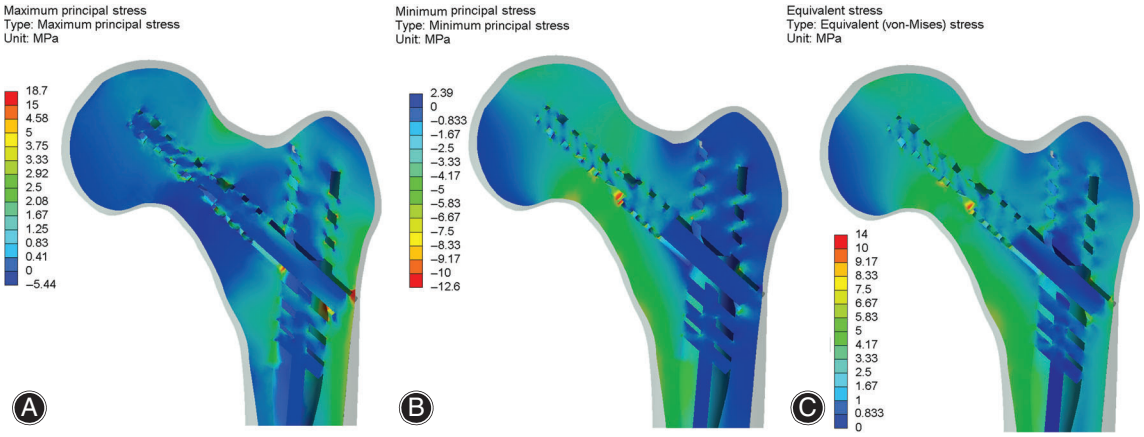

Fig. 9 The maximum principal stress distribution (A), minimum principal stress distribution (B), and von Mises stress distribution (C) of the proximal femur model at 12 months postoperatively with biodegradable Mg alloy bionic Gamma nail implanted.

nails and biodegradable magnesium alloy bionic Gamma nails. Our results showed that traditional titanium alloy Gamma nails change the stress distribution of the proximal femoral cancellous bone as compared with the intact model. The main reason is that high implant stiffness transmits the stress from the bone to the screw, which increases the stress shielding effect of the bone. However, compared with traditional metal materials, using biodegradable materials can significantly reduce stress concentration. One reason may be that the process of material degradation will reduce the stiffness of the implants and reduce the high stress value of the implant junction[23]. Tsuang *et al.*[30] used biodegradable materials for posterior spinal fixation; the results showed that when the material degenerated, the same load would increase the deformation of the rod body and reduce the stress concentration. The present study also found that with the degradation of the magnesium alloy, the stress distribution in the proximal femur became closer to that of the intact bone.

Role of Magnesium Alloy in Orthopaedics

Metal materials play an important role in orthopaedic repair and reconstruction. At present, most implants are made of titanium alloy or other metal materials[31], whose elastic modulus does not match the elastic modulus of normal human bones. A higher elastic modulus will produce a stress shielding effect during fracture healing. Long-term implantation will reduce the surrounding bone density, which is not conducive to fracture healing[32], and it is difficult to remove after bone healing. As an implant material with great potential, magnesium can overcome the shortcomings of existing metal materials. The elastic modulus of magnesium is most similar to that of human bones; therefore, using it can avoid the influence of the stress shielding effect on the formation and shaping of new bone[33]. In addition to the ability of magnesium alloys to provide mechanical stability, the degradation of Mg^{2+} also contributes to bone regeneration[34,35]. The biodegraded magnesium material can be dissolved after healing without the need for a second surgery to remove the implant, thereby avoiding additional surgical trauma. These characteristics make magnesium alloys an ideal bone implant material. However, the problems of rapid degradation of magnesium alloys and gas production can lead to the failure of internal fixation[36]. However, the corrosion resistance of magnesium alloy materials has been greatly improved. Therefore, implant materials now have good biocompatibility and durable mechanical integrity in clinical orthopaedics[37].

Limitations of the Study

Although our research revealed the biomechanical advantages of bionic implants using finite element analysis, this study does have limitations. First, the material properties of cortical bone, cancellous bone, and implants are assumed to be isotropic, linear elastic, and homogeneous, which may lead to errors in the experimental results. Second, for biodegradable magnesium implants, we ignored the volume change and assumed that the Young's modulus decreases with time. In addition, only one type of intertrochanteric fracture was considered in our study.

Conclusion

With the biodegradable magnesium alloy bionic implant, the stress distribution of the fractured bone is closer to the stress distribution of the intact bone and the implant does not need to be removed, thereby aiding in protecting the healing bone and restoring the bone structure. Therefore, the biomimetic Gamma nail system made of biodegradable magnesium alloy has promising clinical value.

ACKNOWLEDGMENTS

The authors are grateful to the Institute of Orthopaedic Research of Hebei Province for their excellent technical support.

References

1. Chen W, Lv H, Liu S, *et al*. National incidence of traumatic fractures in China: a retrospective survey of 512 187 individuals. Lancet Glob Health, 2017, 5: e807–e817.
2. Yu J, Zhang C, Li L, *et al*. Internal fixation treatments for intertrochanteric fracture: a systematic review and meta-analysis of randomized evidence. Sci Rep, 2015, 5: 18195.
3. Yoo J, Kim S, Choi J, Hwang J. Gamma 3 U-blade lag screws in patients with trochanteric femur fractures: are rotation control lag screws better than others? J Orthop Surg Res, 2019, 14: 440.
4. Pascarella R, Fantasia R, Maresca A, *et al*. How evolution of the nailing system improves results and reduces orthopedic complications: more than 2000 cases of trochanteric fractures treated with the Gamma Nail System. Musculoskelet Surg, 2016, 100: 1–8.
5. Stiehl JB, Jacobson D, Carrera G. Morphological analysis of the proximal femur using quantitative computed tomography. Int Orthop, 2007, 31: 287–292.
6. Kumar P, Rajnish RK, Sharma S, Dhillon MS. Proximal femoral nailing is superior to hemiarthroplasty in AO/OTA A2 and A3 intertrochanteric femur fractures in the elderly: a systematic literature review and meta-analysis. Int Orthop, 2001, 44: 623–633.
7. Omari A, Madsen CM, Lauritzen JB, Jørgensen HL, Vojdeman FJ. Comorbidity and mortality after hip fracture in nineteen thousand six hundred and eighty two patients aged eighteen to sixty five years in Denmark from 1996 to 2012. Int Orthop, 2019, 43: 2621–2627.
8. Forni C, Gazineo D, D'Alessandro F, *et al*. Predictive factors for thirty day mortality in geriatric patients with hip fractures: a prospective study. Int Orthop, 2019, 43: 275–281.
9. Holzer G, Skrbensky G, Holzer LA, Pichl W. Hip fractures and the contribution of cortical versus trabecular bone to femoral neck strength. J Bone Miner Res, 2009, 24: 468–474.
10. Richmond J, Aharonoff GB, Zuckerman JD, Koval KJ. Mortality risk after hip fracture. J Orthop Trauma, 2003, 17: 53–56.
11. Siavashi B, Aalirezaei A, Moosavi M, Golbakhsh MR, Savadkoohi D, Zehtab MJ. A comparative study between multiple cannulated screws and dynamic hip screw for fixation of femoral neck fracture in adults. Int Orthop, 2015, 39: 2069–2071.
12. Kasha S, Yalamanchili RK. Management of subtrochanteric fractures by nail osteosynthesis: a review of tips and tricks. Int Orthop, 2020, 44: 645–653.
13. Bartoníček J, Rammelt S. The history of internal fixation of proximal femur fractures Ernst Pohl-the genius behind. Int Orthop, 2014, 38: 2421–2426.
14. Güven M, Yavuz U, Kadioğlu B, *et al*. Importance of screw position in intertrochanteric femoral fractures treated by dynamic hip screw. Orthop Traumatol Surg Res, 2010, 96: 21–27.
15. Glassner PJ, Tejwani NC. Failure of proximal femoral locking compression plate: a case series. J Orthop Trauma, 2011, 25: 76–83.
16. Jin WJ, Dai LY, Cui YM, Zhou Q, Jiang LS, Lu H. Reliability of classification systems for intertrochanteric fractures of the proximal femur in experienced orthopaedic surgeons. Injury, 2005, 36: 858–861.
17. Liu Y, Tao R, Liu F. Mid-term outcomes after intramedullary fixation of peritrochanteric femoral fractures using the new proximal femoral nail antirotation (PFNA). Injury, 2010, 41: 810–817.
18. Horner NS, Samuelsson K, Solyom J, Bjørgul K, Ayeni OR, Östman B. Implant-related complications and mortality after use of short or long Gamma nail for intertrochanteric and subtrochanteric fractures: a prospective study with minimum 13-year follow-up. JBJS Open Access, 2017, 2: e0026.
19. Huang H, Xin J, Ma B. Analysis of complications of intertrochanteric fracture treated with Gamma 3 intramedullary nail. Int J Clin Exp Med, 2014, 7: 3687–3693.
20. Sowmianarayanan S, Chandrasekaran A, Kumar RK. Finite element analysis of a subtrochanteric fractured femur with dynamic hip screw, dynamic condylar screw, and proximal femur nail implants–a comparative study. Proc Inst Mech Eng, Part H, 2008, 222: 117–127.
21. Tsuang FY, Hsieh YY, Kuo YJ. Assessment of the suitability of biodegradable rods for use in posterior lumbar fusion: an in-vitro biomechanical evaluation and finite element analysis. PLoS One, 2007, 12: e0188034.
22. Taheri NS, Blicblau AS, Singh M. Comparative study of two materials for dynamic hip screw during fall and gait loading: titaniumalloy and stainless steel. J Orthop Sci, 2011, 16: 805–813.
23. Cui Y, Dou C, Tian S, *et al*. Traditional and bionic dynamic hip screw fixation for the treatment of intertrochanteric fracture: a finite element analysis. Int Orthop, 2020, 44: 551–559.
24. Tetsunaga T, Fujiwara K, Endo H, *et al*. Calcar femorale in patients with osteoarthritis of the hip secondary to developmental dysplasia. Clin Orthop Surg, 2017, 9: 413–419.
25. Shankar N, Babu SS, Viswanathan C. Bone trabecular analysis of proximal femur radiographs for the detection of osteoporosis using anisotropic Morlet wavelet transform. Cluster Comput, 2019, 22: 14513–14523.
26. Zhang Q, Chen W, Liu HJ, *et al*. The role of the calcar femorale in stress distribution in the proximal femur. Orthop Surg, 2009, 1: 311–316.
27. Nawathe S, Nguyen BP, Barzanian N, Akhlaghpour H, Bouxsein ML, Keaveny TM. Cortical and trabecular load sharing in the human femoral neck. J Biomech, 2015, 48: 816–822.
28. Rachner TD, Khosla S, Hofbauer LC. Osteoporosis: now and the future. Lancet, 2011, 377: 1276–1287.
29. Keaveny TM, Yeh OC. Architecture and trabecular bone-toward an improved understanding of the biomechanical effects of age, sex and osteoporosis. J Musculoskelet Neuronal Interact, 2002, 2: 205–208.
30. Tsuang FY, Hsieh YY, Kuo YJ, *et al*. Assessment of the suitability of biodegradable rods for use in posterior lumbar fusion: an in-vitro biomechanical evaluation and finite element analysis. PLoS One, 2017, 12: e0188034.
31. Niinomi M, Nakai M, Hieda J. Development of new metallic alloys for biomedical applications. Acta Biomater, 2012, 8: 3888–3903.
32. Nagels J, Stokdijk M, Rozing PM. Stress shielding and bone resorption in shoulder arthroplasty. J Shoulder Elbow Surg, 2003, 12: 35–39.
33. Li X, Liu X, Wu S, Yeung KWK, Zheng Y, Chu PK. Design of magnesium alloys with controllable degradation for biomedical implants: from bulk to surface. Acta Biomater, 2016, 45: 2–30.
34. Li HF, Xie XH, Zheng YF, *et al*. Development of biodegradable Zn-1X binary alloys with nutrient alloying elements Mg, Ca, and Sr. Sci Rep, 2015, 5: 10719.
35. Wu L, Feyerabend F, Schilling AF, Willumeit-Römer R, Luthringer B. Effects of extracellular magnesium extract on the proliferation and differentiation of human osteoblasts and osteoclasts in coculture. Acta Biomater, 2015, 27: 294–304.
36. Witte F, Kaese V, Haferkamp H, *et al*. In vivo corrosion of four magnesium alloys and the associated bone response. Biomaterials, 2005, 26: 3557–3563.
37. Liu C, Ren Z, Xu Y, Pang S, Zhao X, Zhao Y. Biodegradable magnesium alloys developed as bone repair materials: a review. Scanning, 2018: 9216314.